Investigation of the Turbulent Shear Flow of Dilute Aqueous CMC Solutions

WILLIAM D. ERNST

Ling-Temco-Vought, Inc., Dallas, Texas

Experimental measurements of the fully developed turbulent flow field in straight circular tubes of dilute CMC solutions are described. The viscosity of the solutions used had a non-Newtonian power law exponent of 0.93 to 0.95 in order to eliminate most of the effects attributed to power law fluids. Both pressure drop and velocity profile measurements were made over a wide range of Reynolds numbers. The velocity data were taken in both the linear sublayer and the turbulent core, and are presented in terms of the universal velocity parameters modified by use of a viscosity defined at the tube wall. A check of the existing empirical correlations based on a power law viscosity shows that none predict the observed velocity profiles.

While most fluids are completely described by the linear relationship between the shear stress and shear rate, called *Newton's law of viscosity,* non-Newtonian fluids have either an additional property or a nonlinear functional relationship between the shear stress and shear rate, or both (*1, 2*). There has been a significant amount of work published on purely viscous non-Newtonian fluids which agrees with the semitheoretical expressions derived (*3, 4*). These fluids appear to have a friction factor vs. Reynolds number dependence that is independent of pipe diameter. The nonlinear functional relation most often used to characterize the properties of a purely viscous liquid is the power relation (*5*):

$$\tau = a\left(\frac{du}{dy}\right)^n \qquad (1)$$

This relation, however, does not describe any of the unequal normal stresses appearing in many fluids.

An elasticoviscous fluid has a non-Newtonian rheology that gives it one of the properties of a solid, elasticity, and may or may not have a nonlinear shear stress versus shear rate relationship (*6* to *8*). Elasticity gives the fluid the ability to store energy reversibly and induces normal stresses. A complete description of a fluid's properties, a constitutive equation, when expressed in a tensor form, must obey certain laws of invariance, making the material constants or properties of the constitutive equation difficult to evaluate experimentally (*9* to *11*). As yet, there is no means of measuring the constants necessary for describing the properties as predicted from the more complete, and therefore, more complicated sets of constitutive equations for elasticoviscous fluids. The only instance of success involves the correlation of the normal stresses in laminar flow with the shear reduction in turbulent flow (*12*). All existing data for fluids which are classified as being elasticoviscous indicate that, unlike the purely viscous fluid, the friction factor vs. Reynolds number correlation is dependent on tube diameter (*4, 13, 14*).

Specifically this report describes an experimental study of dilute (0.05% by weight) concentrations of CMC 7 HSP flowing in tubes of two different diameters (0.650 in. I.D. and 1.427 in. I.D.) with a flow rate between 1.5 and 275 gal./min. Measurements of pressure drop, viscosity, and bulk velocity allowed a calculation of the friction factor for Reynolds numbers, based on a power law viscosity, from 6.0×10^3 to 4.6×10^5. Velocity profiles were determined at six Reynolds numbers in the large pipe and seven in the small pipe (using a probe 0.005 in. thick which allowed measurements close to the wall) in order to test the conventional relationship between ϕ and η, that is, the law-of-the-wall parameters.

In keeping with the fluid mechanics viewpoint, the major effort has been in the determination of velocity profiles so that the radial zone affected by the non-Newtonian properties might be located. As measurements of elasticoviscous flow in the linear sublayer zone have not been made previously, it must be expected that these results are subject to a certain amount of error and further verification. It is not the intention of this report to present conclusive solutions, but rather to clarify the problem and to single out the areas for further study.

At the conception of these tests, the fluid property responsible for the large shear reduction was not known, although there were indications that this property was not the nonlinear, shear stress–shear rate relationship. Therefore, the test fluid was selected on the basis of its linearity. If a fluid could be found which had a linear viscosity and yet reduced the turbulent skin friction, then the property causing the skin friction reduction must be a property other than viscosity. CMC 7 HSP, a high molecular weight cellulose gum of sodium carboxymethelcellulose (*15*), was chosen as the additive used on the basis of its low rate of degradation, nearly linear viscosity ($n \approx 0.94$), ease of mixing, and widespread use in experimental studies.

EXPERIMENTAL APPARATUS AND PROCEDURES

Property Measurements

Since there was no method by which the elastic properties could be determined at the low concentrations used, only the viscosity was measured. This viscosity was found to be slightly nonlinear and is characterized in this article by using the power law approximation. It must be pointed out that this approximation does not include either the normal stresses or elasticity thought necessary to describe the CMC properties completely, but it is the best available.

The Fann Model 35 concentric cylinder, rotational viscometer was used to monitor the fluid viscosity at the test site through-

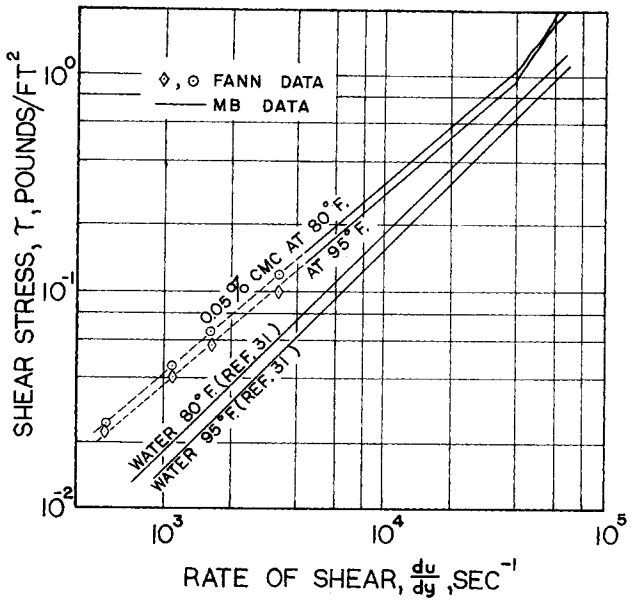

Fig. 1. Comparison of shear stress data taken in the Fann and Merrill Brookfield viscometers.

out the experiments. These measurements were used in the reduction of all the experimental results. The Fann viscometer, which has a usable shear rate range from 542 to 3,252 sec.$^{-1}$, was calibrated throughout the tests with water. The narrow shear rate range necessitated a different viscometer to check the nonlinearity of the viscosity at the higher shear rates experienced in the tests. The Merrill Brookfield High Shear viscometer was used to extend the shear rate range investigated to 70,000 sec.$^{-1}$ (shear rate at which parallel flow breaks down). As shown in Figure 1, the power law relation is valid up to the maximum shear rate at which the shear stress is accurate. Although the maximum shear rate used in the determination of viscosity is less than that produced in the pipe, experimental evidence indicates that for dilute concentrations of some polymer additives, the power law is still valid for shear rates up to 325,000 sec.$^{-1}$ (*16*).

In general, the power law character of the viscosity makes it more imperative to account for the variation of shear rate with radius in the viscometer measurements (*1*). In all instances with the rotor-stator combination used in the Fann viscometer, this variation was neglected, since the shear rate determined from the angular velocity of the outer cylinder deviated less than 1/3 of 1% from the true shear rate. In the Merrill Brookfield viscometer, the deviation was even less and was also neglected.

Figure 1 also shows the relatively small temperature dependence of the dilute solutions used. In most instances, the temperature of the fluid when tested in the Fann viscometer was different from that at which the pipe flow experiment was run. However, the viscosity variation for the small temperature differences present was interpolated linearly with temperature, and it is believed that the error in this method was negligible compared to the accuracy (± 2%) of the overall viscosity determination. Others (*17*) have noted that 30°F. temperature differences in the turbulent flow of dilute CMC solutions have relatively small influence on the shearing resistance.

Degradation of the fluid properties, noted throughout the tube flow experiments, appears to be both shear and time dependent. New solutions were mixed whenever the power law exponent varied by more than 2% from one run to another. The coefficient a in the power law viscosity relation was not controlled, however, and was allowed to vary. This arrangement permitted the same solution to be used as long as three days without change. The variation in the viscosity coefficient with time between test fluid samples was assumed to be linear and was accounted for by interpolation of the typical data presented in Figure 2. While a varied between 3.77×10^{-5} and 5.22×10^{-5}, n varied between 0.93 and 0.95. The actual values of a and n corrected for temperature and degradation are shown in the tabulated velocity profiles.

Facility

The facility used for the tests is essentially a closed-loop system with a stilling tank and flexible hose feeder added to provide smooth, surge-free flow. In order to eliminate any irregularities, the two test sections (0.650 in. I.D. and 1.427 in. I.D.) were polished smooth at the start and periodically during the tests. Fully developed turbulent pipe flow of the non-Newtonian fluid was assured by having one hundred and forty pipe diameters upstream of the test section. The two pressure manometers (a 10-in. null balance micromanometer and a 6-ft. mercury-water U-tube) could be connected across any two of the static pressure taps to provide a check of the pressure drops measured. The checks with water in both pipes at the start of the tests and with CMC in the small pipe throughout the tests indicated no systematic differences between the pressure taps. During the experiments in the large pipe, two sets of pressure taps became inoperative due to the chemical attack of the CMC on the aluminum clad tubing, and prevented a check of the pressure data in that pipe. Three flowmeters with an accuracy of ± 2%, except at the very lowest flow rates, were used to cover the range of flow rates used.

Instrumentation

In order to measure velocities inside the sublayer, a probe of small dimensions was needed. This probe consisted of five telescoping stainless steel tubes with the smallest tube (0.012 in. I.D.) hammered and filed flat to give a 0.006 in. by 0.030 in. tip. The radial position of the probe tip in the pipe was indicated by a depth micrometer which measured the displacement of the probe tip from the point where it made electrical contact with the wall. The overall error in the determination of the probe position is believed to be less than 0.0005 in.

A differential pressure transducer was used to determine the dynamic pressure in order to reduce the time to take the velocity readings. The pressure transducers were calibrated with a micromanometer having 0.0002 in. of water sensitivity and a secondary standard mercury manometer. The overall error in the velocity instrumentation system was determined to be less than ± ¾%. Several capacitors were used in the output circuit to eliminate fluctuations in the pressure readings.

Since the most important measurements were of fluid velocity, the experimental procedure was designed to minimize any errors which might be present in the velocity instrumentation. After first adjusting the flow rate to the desired value and allowing the fluid temperature to stabilize, the facility was shut down and the zero differential pressure on the transducer was read. Then the flow was started and allowed to stabilize before an

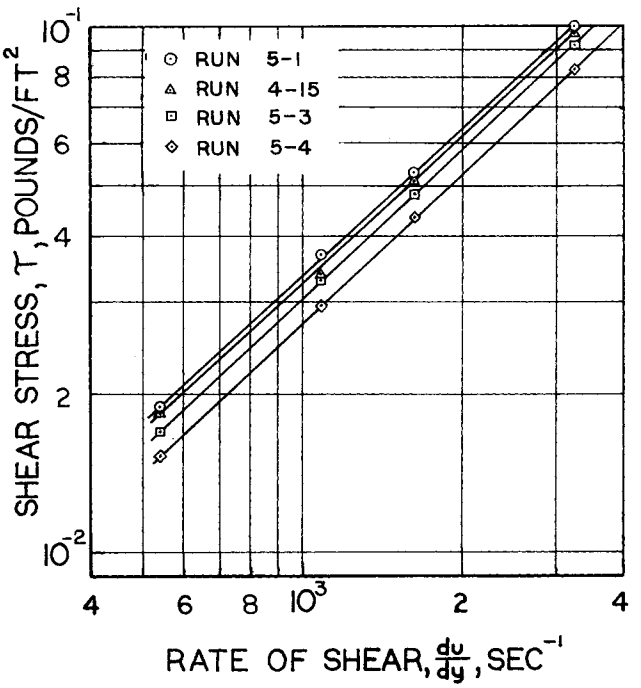

Fig. 2. Typical low shear rate data for test solutions.

electrical indication of the wall position was made. The velocity profile, pressure drop, flow rate, and the temperature were then measured simultaneously. If there were any appreciable differences in any of the last three of these quantities, the run was discarded and repeated at a later time. The viscosity was measured after every 4 hr. of running, and the fluid viscosity at intermediate times was interpolated linearly from these data.

RESULTS AND DISCUSSION

There have been several experimental programs performed previously (*3, 4, 17*) to determine the turbulent and laminar flow characteristics of more concentrated CMC solutions. The large differences in fluid properties, however, prevent any close comparisons of experimental results. Even in instances where the same concentrations of a single polymer additive are used, the fluid viscosity is most often different and dependent upon the solvent purity (*18*). In addition, the fluid elasticity may be affected by the solvent purity in a manner that is different from that of the viscosity. Also, since the effects of tube diameter are unknown, no comparisons can be made between data taken in tubes of different sizes. These effects have prevented the cross checking of experimental results, and for this reason all of the data reported herein are for a single fluid viscosity index within experimental limitations.

Basically, the problem of specifying the correlation of the turbulent friction factor with the Reynolds number resolves itself into two dependent parts: first, the determination of the complete relation between shear stress and shear rate; second, the determination of velocity as a function of radial position in terms of universal constants. Universal constants are those which can be determined experimentally and can be applied to a physical boundary-layer flow field independent of fluid type, free stream velocity, and surface geometry. These two processes will now be considered in detail.

At present, the fluid properties that can be measured are incomplete since they neglect elasticity, and the power law relation used is, at best, only an approximation for the viscous properties. However, this viscosity characterization worked reasonably well for friction factor prediction in laminar flow (*5*) and therefore was extended to turbulent flow. In addition, the power law was used to change several parameters in the universal velocity correlation, $u/u^* = A \log_{10} u^*y/\nu + D$, known as the law-of-the-wall, which was expected to predict the correct velocity profiles. Since the power law viscosity changes with radial distance (shear rate), in the past it was thought necessary to account for this effect in all the turbulent velocity correlations (*4, 19, 20*). This changed the usual parameter for the radial change of velocity, yu^*/ν, to $\rho\, y^n u^{*2-n}/a$, which made the theoretical velocity gradient vary as a function of n. However, in turbulent flow, viscosity is most important at the wall and serves as a reference parameter only for the remaining velocity field, since the momentum is transferred through the fluid by a macroscopic process rather than a microscopic process. Therefore the usual law-of-the-wall parameters were used with only the viscosity modified, as shown below.

The original formulation of the law-of-the-wall was based on experimental observations in a pipe, dimensional analysis, and the formulation of some simple similarity laws (*21*). This formulation is based on the shear velocity $u^{*2} = \tau_w/\rho$ at the wall, and to be consistent within the assumption of the similarity laws, the viscosity must also be determined at the wall. Therefore, by defining

$$\nu_w = \frac{\tau_w}{\rho (du/dy)_w} \qquad (2)$$

and by assuming that the power law applies at the wall

$$\tau_w = a \left(\frac{du}{dy}\right)_w^n$$

we have, after substitution,

$$\nu_w = \frac{\tau_w^{1-1/n}\, a^{1/n}}{\rho}$$

This value of viscosity at the wall was used in the reduction of all the velocity data to the universal form.

By using the universal velocity correlations with the constants A and D determined experimentally, Prandtl (*22*) found it was possible to derive the friction factor vs. Reynolds number relationship. Nikuradse (*23*), by using his experimental results to modify slightly the constants derived for this relation, predicted all the experimental data up to a Reynolds number of 3×10^6. This relation is used later for the comparison of experimental data with Newtonian theory.

Although the Reynolds number could be based on the ν_w, at the present it is better for two reasons to continue with the existing power law Reynolds number $N_{Ren} = 8[2(3 + 1/n)]^{-n} [\rho\, d^n\, \bar{u}^{2-n}/a]$, derived from laminar flow considerations (*5*). First, all of the previous experimental data have been presented and compared on this basis and a different Reynolds number would only increase the present confusion of experimental results. Second, the ν_w presupposes knowledge of the τ_w which is the quantity that the correlation should predict. Therefore, the universal velocity data will be presented in terms of ν_w, while the friction factor vs. Reynolds number data will be presented in terms of N_{Ren}.

Velocity Measurements

As mentioned previously, the velocity data are subject to four errors of measurement and each of these will be considered before discussion the velocity results. At low probe Reynolds numbers, the viscous action of the fluid increases the stagnation point pressure and a total pressure probe gives a false indication of the stagnation pressure. At the lowest velocity used in these tests, the tip Reynolds number based on the probe tip height is approximately 50 which makes the velocity indicated by the probe approximately 0.5% low (*24*). The effect of the large velocity gradients close to the wall is to displace the point at which the true stagnation pressure is measured away from the wall (*25*). This phenomenon serves to increase the velocity actually measured. For the probe dimensions used, the effective center of the probe should be displaced by approximately 0.001 in. The expected turbulence level also serves to increase the dynamic pressure measured at the probe tip, thereby increasing the velocity slightly (*26*). Finite static tap diameter increases the static pressure (*27, 28*) and thus reduces the measured velocity by less than 0.5%. Overall, the expected probe and tap diameter effects would tend to decrease the integrated flow rates by less than 0.5%, while the velocity close to the wall would be increased slightly.

The forementioned results are based on experimental results obtained from measurements on Newtonian fluids. In particular, most of the possible effective center corrections have been justified by agreement with the hypothesized linear sublayer, but no such hypothesis has been demonstrated experimentally for non-Newtonian fluids. Therefore, it was decided not to make any adjustment of the data and to present the original data for individual interpretation.

All of the velocity data† are presented in terms of the

† The velocity profiles presented herein are typical of those taken. A tabulation of all the velocity data has been deposited as document 8769 with the American Documentation Institute, Photoduplication Service, Library of Congress, Washington 25, D. C., and may be obtained for $2.50 for photoprints or $1.75 for 35-mm. microfilm.

turbulent boundary layer parameters ϕ and η. The solid line on each plot is the empirical expression for the turbulent Newtonian flow of fluids proposed by Coles (29), $\phi = 5.75 \log_{10} \eta + 4.5$. Figure 3 ($N_{Ren} = 3.87 \times 10^4$) shows a typical profile for water. As none of the corrections discussed earlier have been made, there is a tendency for the displacement of the probes effective center away from the wall to indicate a greater velocity than that actually present. A displacement of the effective center by only 0.002 in. would give excellent agreement between the velocity profile and the empirical curve. Figures 3 and 4 present the typical results of the measurement of turbulent velocity profiles of 0.05% CMC in the large pipe and small pipe, respectively. The ϕ, η relationship is based on the assumption that there are three different regions of flow as indicated by the curve. For $\eta > 30$, the flow is fully turbulent and the effect of viscosity is negligible. For $\eta < 8$, the flow is essentially linear and viscosity predominates. The third region is a buffer zone between the other two.

Looking first at the fully turbulent region, the most significant effect is the parallel shift of the velocity by as much as 28% at the highest N_{Ren}. From the phenomenological point of view, the parallel shift means that the mixing length remains unchanged by the elasticoviscous properties of the fluid, since the coefficient of $\log_{10} \eta$ is dependent on the mixing length. This shift indicates that a fluid property in addition to viscosity is needed to correlate the data if the mixing length concept is correct. Also, since the magnitude of the shift is dependent on N_{Ren}, any correlating parameter must be a function of the flow field as well.

When a plot is made in terms of the velocity defect law, $(u_m - u)/u^* = f(2y/d)$, the 0.05% CMC solutions agree well with the empirical relationship for Newtonian fluids. This is to be expected, since the mixing length parameter k is unchanged.

From a physical point of view, the constant slope with increasing N_{Ren} implies that the mechanism of turbulent momentum transport remains the same and is independent of N_{Ren}. The decrease in magnitude of the turbulent mixing as reported by Metzner (4) must then have only a small effect on the rates of momentum transport at these small concentrations.

The velocity profiles for the small pipe will be examined first for overall trends, since this set of data has both the greatest N_{Ren} range and accuracy (Figure 4). The linear region close to the wall displays no deviation from that expected for Newtonian fluids at low N_{Ren}. Actually, at $N_{Ren} = 1.33 \times 10^4$, the velocity data, which are uncorrected for displacement of effective center, show a better agreement with the Newtonian correlation than the uncorrected zero concentration measurements, implying that the net velocity correction may be smaller for elasticoviscous fluids. If one looks closely at the region between $\eta = 8$ and $\eta = 30$ for $N_{Ren} = 6.99 \times 10^4$, it appears that the velocity in the buffer zone is uniformly displaced in proportion to that in the fully turbulent region. This somewhat unexpected result would seem to indicate that the significant effect of the elasticoviscous fluid properties is felt in the linear sublayer next to the wall. If one hypothesizes that the linear sublayer remains unchanged by the elasticoviscous properties, then the velocity in the buffer zone should become asymptotic to the linear sublayer velocity at small η. This did not happen as shown above and there could be several reasons why it did not. First, the velocity indicated by the probe may be incorrect. Second, the major elasticoviscous effect may truly be in the linear sublayer. There is much evidence (30) to suggest that the linear sublayer is not laminar at all but is composed of longitudinal and transverse oscillations close to the wall. If this were true, it might explain why the steady laminar flow fields of elasticoviscous fluids can be predicted, and the linear sublayer flow fields of turbulent flow at higher Reynolds numbers cannot.

The tabulated velocity profiles not plotted but intermediate between $N_{Ren} = 6.99 \times 10^4$ and 2.11×10^5 show a continuing increase in the upward displacement of the velocity profile. There is no indication from the available data that this increasing displacement will not continue for even larger N_{Ren}.

The large pipe shows much the same effect; however, the data are over a more limited range (Figure 3). At $N_{Ren} = 9.80 \times 10^4$, the same uniform displacement of the velocity profile in the buffer region is noted.

When the constant D in the law-of-the-wall relationship for the two pipe sizes is compared vs. N_{Ren}, as in Figure 5, the differences between the flow in the different size pipes can readily be seen. The differences correspond exactly with that which is observed in the f vs. N_{Ren} correlation, since the friction factor is an inverse function of D. At high N_{Ren}, the friction factor for the small pipe is less than that of the large pipe, while at lower N_{Ren}, it is essentially the same. Based on Figure 5, it is easy enough to predict what will happen in these sizes of pipe with this particular fluid, but such a correlation without additional data would be useless for extrapolation to other fluid concentrations or pipe sizes, and is therefore omitted.

The velocity profiles obtained show no agreement with the semitheoretical results predicted by Granville, Dodge, and Metzner, and by Clapp for power law fluids, thereby indicating again the presence of elasticity or some additional property other than a nonlinear viscosity.

Friction Factor Measurements

Shown in Figure 6 is the experimental determination of the friction factor vs. N_{Ren} correlation for both water

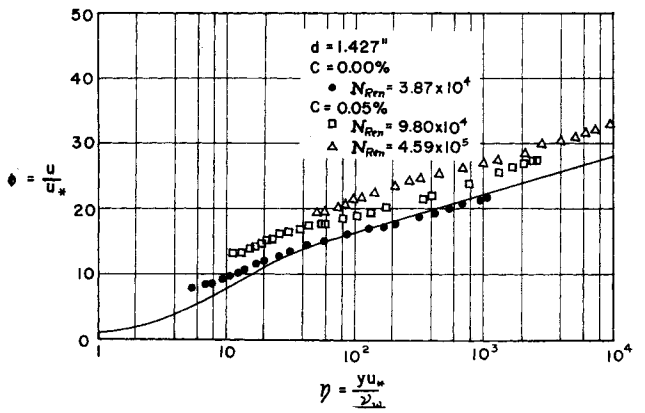

Fig. 3. Typical generalized velocity profiles.

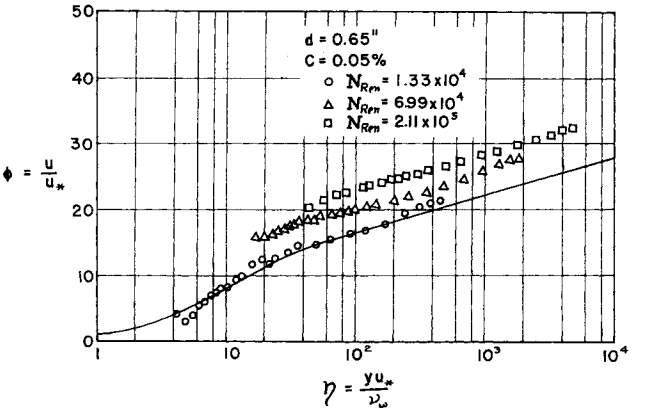

Fig. 4. Typical generalized velocity profiles.

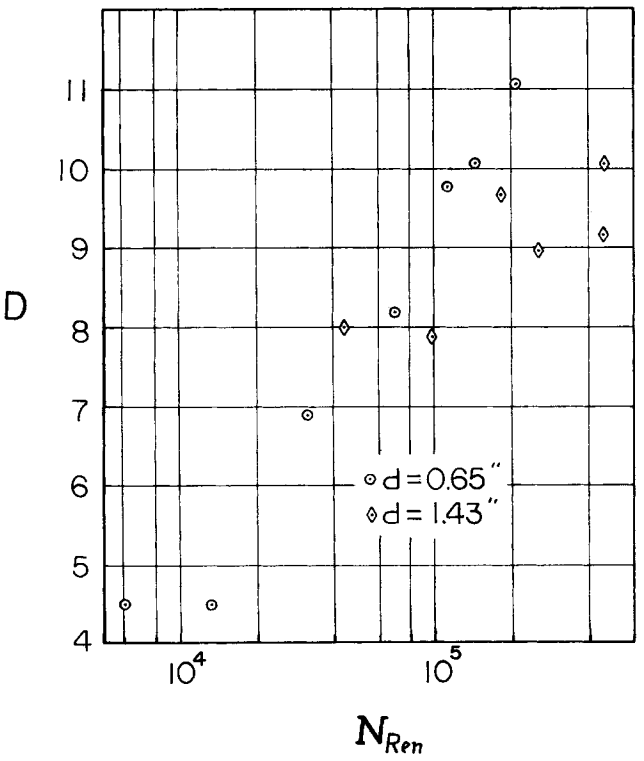

Fig. 5. Comparison of D for small and large tubes as a function of Reynolds numbers.

and the 0.05% CMC solutions for both pipes. The Reynolds number for the test runs with water were determined from the flowmeter readings since there were no velocity profiles taken. All of the data with CMC were based on the integrated velocity profiles, since these profiles were considered the most reliable piece of information taken from the tests. Except for several very low flow rates on 3/8 Pottermeter, which were discarded, all of the integrated profiles showed an average increase in flow rate 7% greater than that indicated by the flowmeters. This effect is as yet unexplained but it is interesting to note that others (*17*) who used a different type of flowmeter and higher concentrations have observed the same variation. Although the maximum reduction in skin friction is not insignificant, it is small compared to what is usually obtained at higher concentrations. However, the purpose of this study was to obtain a liquid having a power law index n as close to one (Newtonian) as possible in order to separate elastic effects from viscous effects. None of the existing power law turbulent flow correlations predicts the curves measured. There does not appear to be any

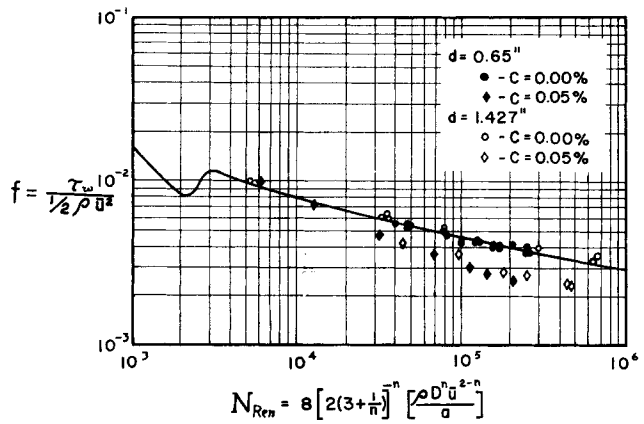

Fig. 6. Friction factor vs. Reynolds number.

appreciable increase in the transition Reynolds number even though the data does not completely cover this range.

In the large pipe, the difficulties with the pressure taps makes the accuracy of both the water and CMC data questionable, but the results as presented are believed to be reasonably accurate. A best fit straight line through the large pipe CMC data would be more parallel to the Newtonian curve than a similar line drawn through the small pipe data.

CONCLUSIONS

The following conclusions may be drawn from the experimental data presented:

1. The decrease in friction factor from the Newtonian value with decreasing pipe diameter is as reported experimentally elsewhere.

2. For the low CMC concentrations used, the friction factor indicates no large increase in the Reynolds number for transition.

3. The major effect of the CMC solutions is a shift linearly upward (increasing with N_{Ren}) of the velocity parameter in the universal law-of-the-wall relationship. This indicates that the mixing length constant has not been affected by the elasticoviscous properties.

4. The lack of agreement with the correlations proposed for pseudo plastic or power law fluids indicates that there is an additional property required to fully describe its motion.

5. Because of the very fundamental differences observed in the velocity profiles, further work is needed to determine how the turbulent momentum transport is modified and to determine the effects of the normal stresses on the measured velocity profiles.

ACKNOWLEDGMENT

The work reported here is part of a project supported jointly by independent research and development funds of Ling-Temco-Vought, Inc., and the National Aeronautics and Space Administration under Contract No. NASw-729 (Fluid Physics Branch of Research Division, OART).

NOTATION

a = non-Newtonian fluid property, defined by Equation (1)
A = dimensionless constant in universal velocity correlation
C = concentration, percent by weight
d = pipe diameter
D = dimensionless constant in universal velocity correlation
f = friction factor, $2\tau_w/(\rho\bar{u}^2)$
n = non-Newtonian fluid index, defined by Equation (1)
Q = flow rate
r = radial coordinate, distance from the tube centerline
N_{Ren} = power law Reynolds number
u = velocity in the x direction
u_m = velocity at the centerline
$\bar{u}$ = bulk velocity, $4Q/(\pi d^2)$
u^* = friction velocity, $(\tau_w/\rho)^{1/2}$
y = normal coordinate, distance from the wall

Greek Letters

τ_w = shear stress at the wall
ρ = density
ϕ = nondimensional velocity (u/u^*)
η = nondimensional normal coordinate (yu^*/ν_w)

ν = viscosity
ν_w = viscosity, defined by Equation (2)

LITERATURE CITED

1. Wilkinson, W. L., "Non-Newtonian Fluids," Pergamon Press, New York (1960).
2. Metzner, A. B., "Handbook of Fluid Dynamics," Chap. 7, McGraw Hill, New York (1961).
3. Shaver, R. G., and E. W. Merrill, *A.I.Ch.E. J.*, **5**, 181 (1959).
4. Dodge, D. W., and A. B. Metzner, *ibid.*, 189.
5. Metzner, A. B., and J. C. Reed, *ibid.*, **1**, 435 (1955).
6. Oldroyd, J. G., *Proc. Roy. Soc. (London)*, **A245**, 278 (1958).
7. Walters, K., *Quart. J. Mech. Appl. Math.*, **15**, 63 (1962).
8. Rivlin, R. S., and J. L. Ericksen, *J. Rational Mech. Anal.*, **4**, 323 (1955).
9. Coleman, B. D., and W. Noll, *Ann. N. Y. Acad. Sci.*, **89**, 672 (1961).
10. Rivlin, R. S., *J. Rational Mech. Anal.*, **4**, 681 (1953).
11. Truesdell, C., *Trans. Soc. Rheol.*, **4**, 9 (1960).
12. Metzner, A. B., and M. G. Park, *J. Fluid Mech.*, **20**, 291 (1964).
13. Savins, J. G., *Soc. Petrol. Eng. J.*, **4**, (3), 203 (1964).
14. Wells, C. S., *Am. Inst. Aeronaut. Astronaut. J.*, **3**, (10), 1800 (1965).
15. Anon., "Hercules Cellulose Gum—Properties and Use," Hercules Powder Co., Wilmington, Del. (1960).
16. Crawford, H. R., private communication to the author.
17. Ripkin, J. F., and M. Pilch, *St. Anthony Falls Hydraulic Lab. Tech. Paper 42, Ser. B* (1963).
18. Ernst, W. D., *A.I.Ch.E. J.*, **11**, (5), 940 (1965).
19. Clapp, R. M., *Inter. Develop. Heat Transfer*, **3**, 652 (1961).
20. Granville, P. S., *David Taylor Model Basis Rept. 1579* (1962).
21. Schlichting, Hermann, "Boundary Layer Theory," McGraw Hill, New York (1960).
22. Prandtl, L., *Aerodynamic Theory, III*, 142 (1935).
23. Nikuradse, J., *VDI Forschungsheft*, **356** (1932).
24. MacMillan, F. A., *J. Roy. Aero. Soc.*, **58**, 837 (1954).
25. Young, A. D., and J. N. Maas, *Aero. Res. Comm. R & M 1770* (1936).
26. Goldstein, S., *Proc. Roy. Soc. (London)*, **A155**, 570 (1936).
27. Shaw, R., *J. Fluid Mech.*, **7**, 550 (1960).
28. Rayle, R. E., S.M. thesis, Mass. Inst. Technol., Cambridge (1949).
29. Coles, D., Ph.D. thesis, California Inst. Technol. (1953).
30. Sternberg, J., *J. Fluid Mech.*, **13**, 241 (1962).
31. Hodgman, C. D., ed., "Handbook of Chemistry and Physics," 32 ed., p. 1827, Chemical Rubber Publishing Co., Cleveland, Ohio (1950).

Manuscript received July 23, 1965; revision received December 27, 1965; paper accepted January 3, 1966.

Local Thermodynamic Consistency of Vapor-Liquid Equilibrium Data for Binary and Multicomponent Systems

F. D. STEVENSON and V. E. SATER

Iowa State University, Ames, Iowa

The Gibbs-Duhem equation, integrated over specific concentration ranges, is used to determine local thermodynamic consistency of vapor-liquid equilibrium data. Several specific applications of the test are given for binary systems, although the method is equally applicable to linear paths in multicomponent systems. The test is particularly useful for evaluating the consistency of incomplete data, that is, data measured over only part of the concentration range.

Since the introductory work of Herington (*1*) and Redlich and Kister (*2*), Prausnitz and Snider (*3*), Van Ness (*4*), and others have extended the applicability of the Gibbs-Duhem equation to test the internal consistency of vapor-liquid equilibrium data for linear paths in multicomponent systems. A test, not restricted to linear paths, was proposed by Li and Lu (*5*) for ternary systems and more recently was extended to multicomponent systems by McDermott and Ellis (*6*). Both the Van Ness and the Li and Lu approaches test for local consistency of the data as well as their overall consistency. A unified consistency test, proposed by Tao (*7*), tests local and overall consistency in binary and multicomponent systems, with consistency or inconsistency being established in terms of the limits of the experimental error of the data. This method, however, becomes relatively insensitive to local inconsistencies at high concentrations when inconsistencies or extrapolation errors at low concentrations are significant.

The purpose of this work is to illustrate the utility, as a precise test for local consistency, of a simple integration of the Gibbs-Duhem equation over a narrow concentration range with the extent of deviation from the null value being an indication of the local inconsistency of the data.

V. E. Sater is at Arizona State University, Tempe, Arizona.